Supporting Information

Non-hydrostatic pressure induced α to β phase transition in group IV-VI Monochalcogenide GeSe

Abliz Mattursun,[#,†] Wenyi Tong,[#,†] Yaqiong Wang,[,†] Zhao Guan,[†] Yonghui Zheng,[†] Wenming Qi,[‖] Jiahao Huang,[†] Lei Yang,[†] Wencheng Fan,[†] Luqi Wei,[†] Yating Xu,[†] Yan Cheng,[†] Pinghua Xiang,[†,§] Binbin Chen,[†] Zhongming Wei,[*,‡] Chungang Duan,[†,§] Ni Zhong[*,†,§]*

[†] Key Laboratory of Polar Materials and Devices (Ministry of Education), Shanghai Center of Brain-inspired Intelligent Materials and Devices, Department of Electronics, East China Normal University, Shanghai 200241, China

[‖]School of physical science and technology, Xinjiang, Xinjiang University, Urumqi 830046, China

[‡]State Key Laboratory of Superlattices and Microstructures, Institute of Semiconductors, Chinese Academy of Sciences; Beijing 100083, China

[§]Collaborative Innovation Center of Extreme Optics, Shanxi University; Taiyuan, Shanxi 030006, China

Email: nzhong@ee.ecnu.edu.cn; yqwang@phy.ecnu.edu.cn; zmwei@semi.ac.cn

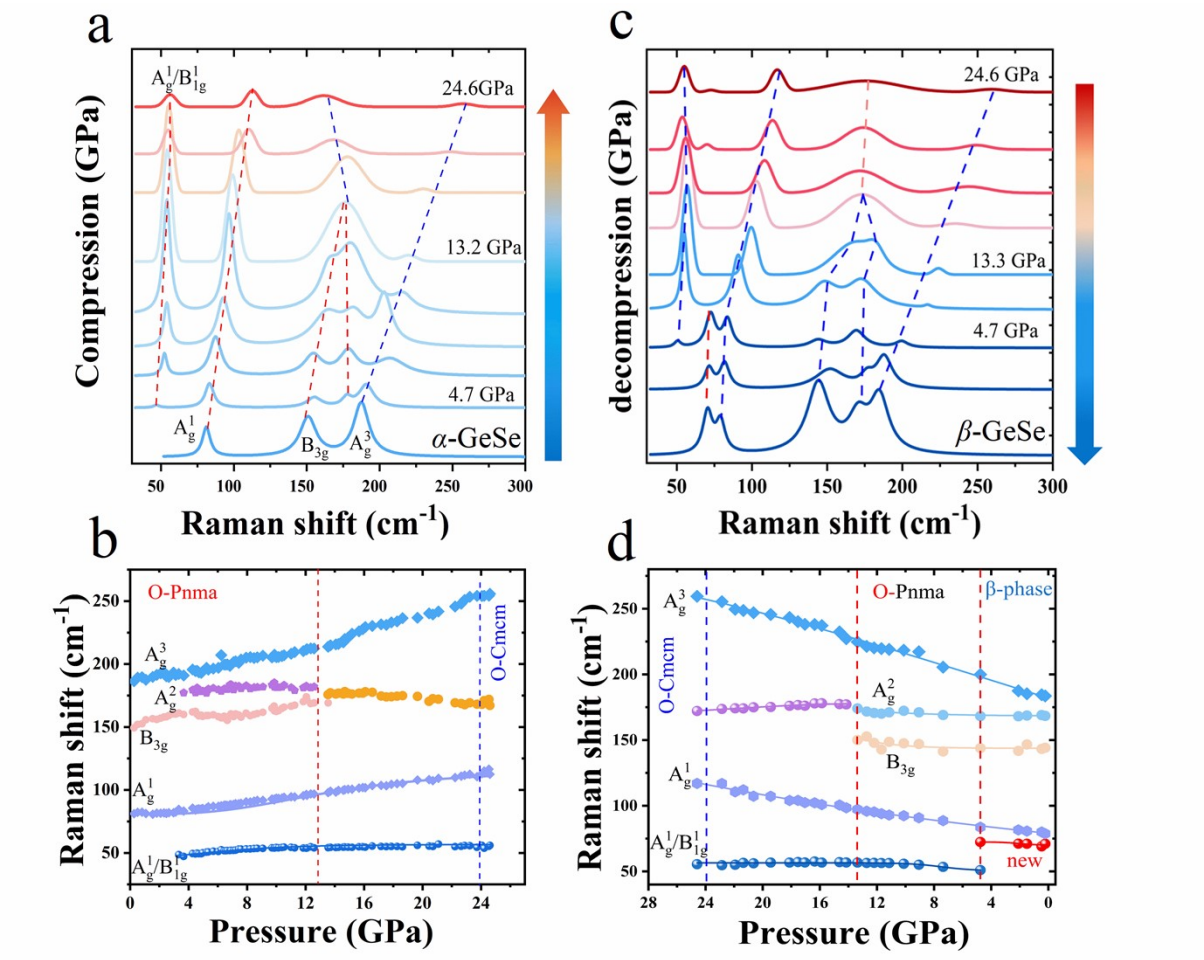

Figure S1. *In situ* Raman spectroscopy results. (a) Raman spectra of α-GeSe from ambient pressure to 24.6 GPa (λ = 532 nm). (b) Pressure-dependence Raman modes from ambient pressure to 24.6 GPa. (c) Decompression dependent of Raman spectra α-GeSe from 24.6 GPa to ambient pressure. (d) Decompression-dependence of Raman modes from 24.6 GPa to ambient pressure. The red dashed line indicates the emergence of a new Raman mode upon decompression.

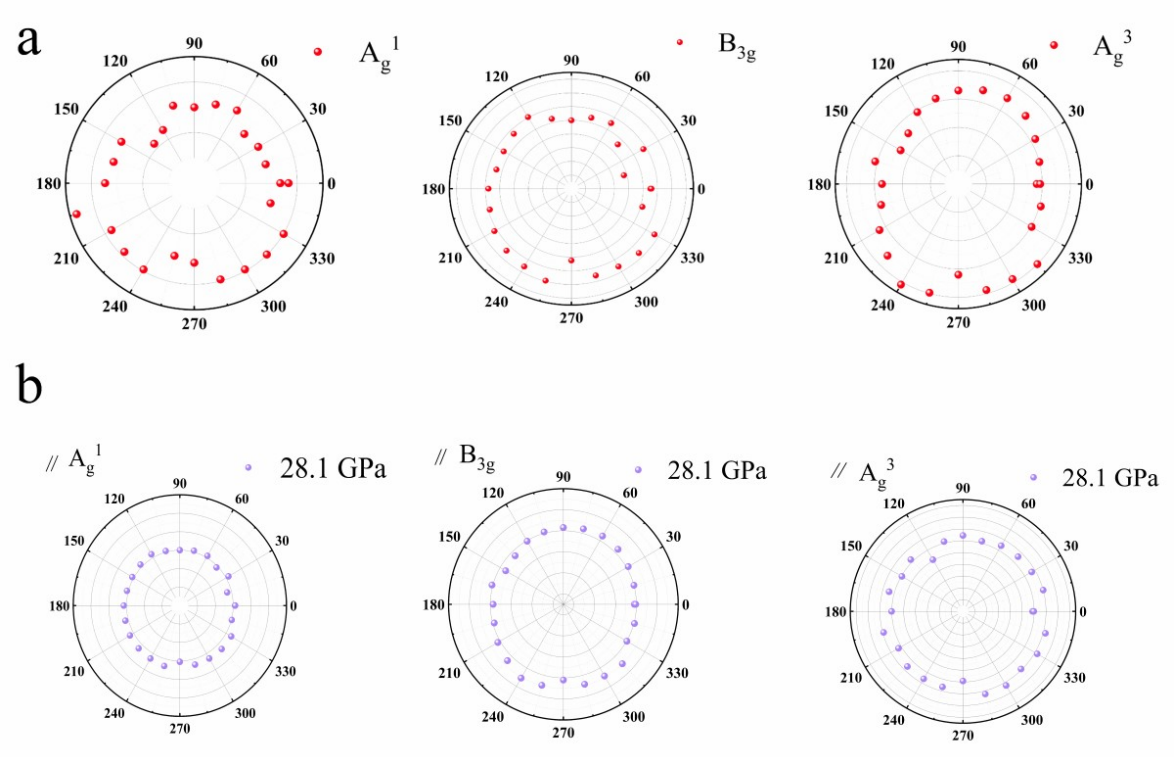

Figure S2. Angle-resolved Raman scattering intensities of A_g^1 ,B_{3g} and A_g^3 modes under pressure 28.1 GPa. (a) Angle-resolved Raman scattering intensities under non-polarization configurations. (b) Angle-resolved Raman scattering intensities under parallel polarization configurations .

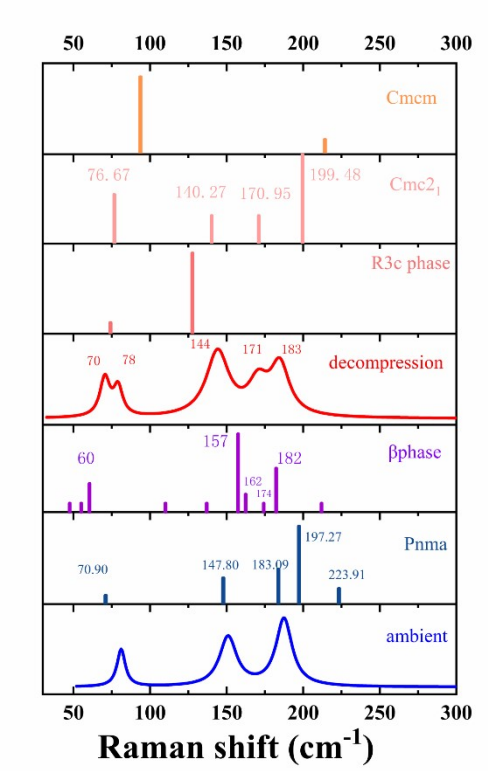

Figure S3. The Raman modes of the *α-Pnma* phase and new phase obtained through theoretical calculations, compression with the Raman spectra under ambient pressure and after decompression from 28.12 GPa. The experimental results represent the Raman mode, and the theoretical calculation results represent the position of the Raman mode.

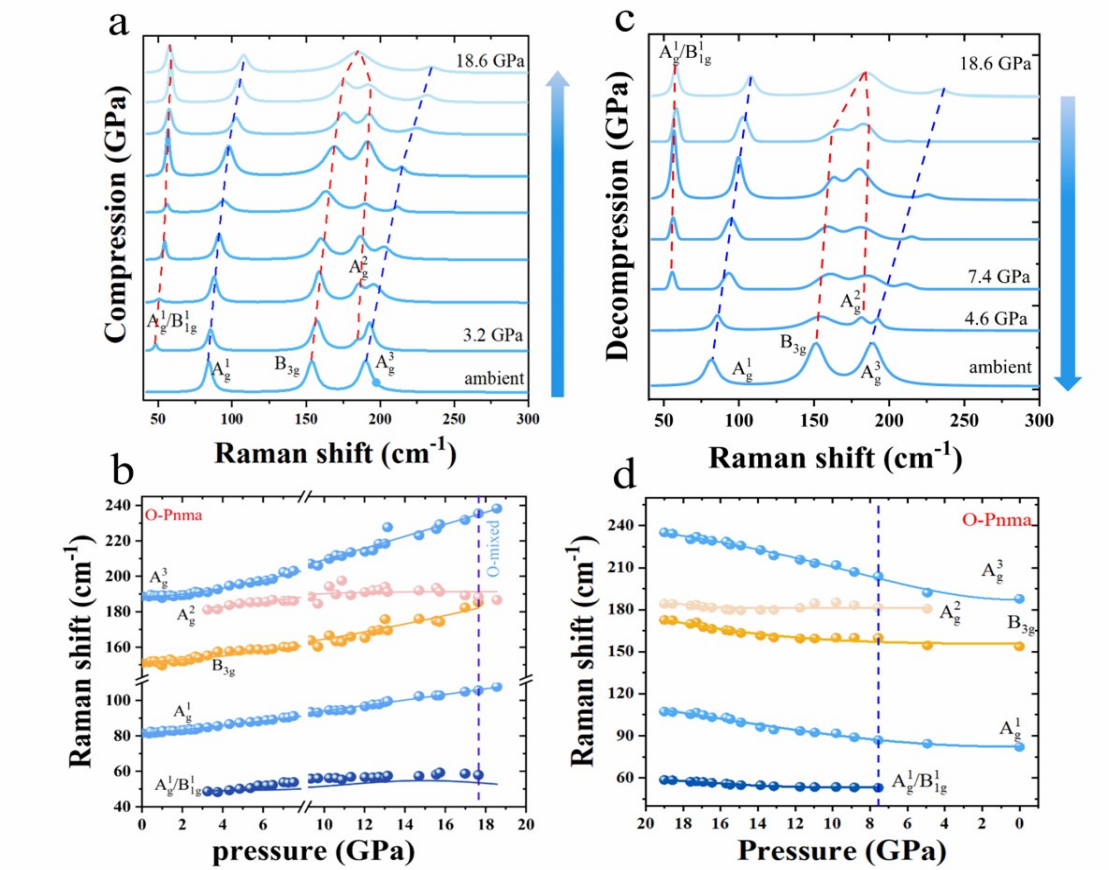

Figure S4. *In situ* Raman spectroscopy results, NaCl as pressure transmission medium. (a) high-pressure Raman spectra of *α*-GeSe from ambient pressure to 18.6 GPa. NaCl as pressure transmission medium. (b) Pressure-dependent Raman modes from ambient pressure to 18.6 GPa. (c) Decompression-dependent Raman spectra of *α*-GeSe from 18.9 to ambient pressure. (d) Decompression-dependence of Raman modes from 18.9 GPa pressure to ambient pressure.

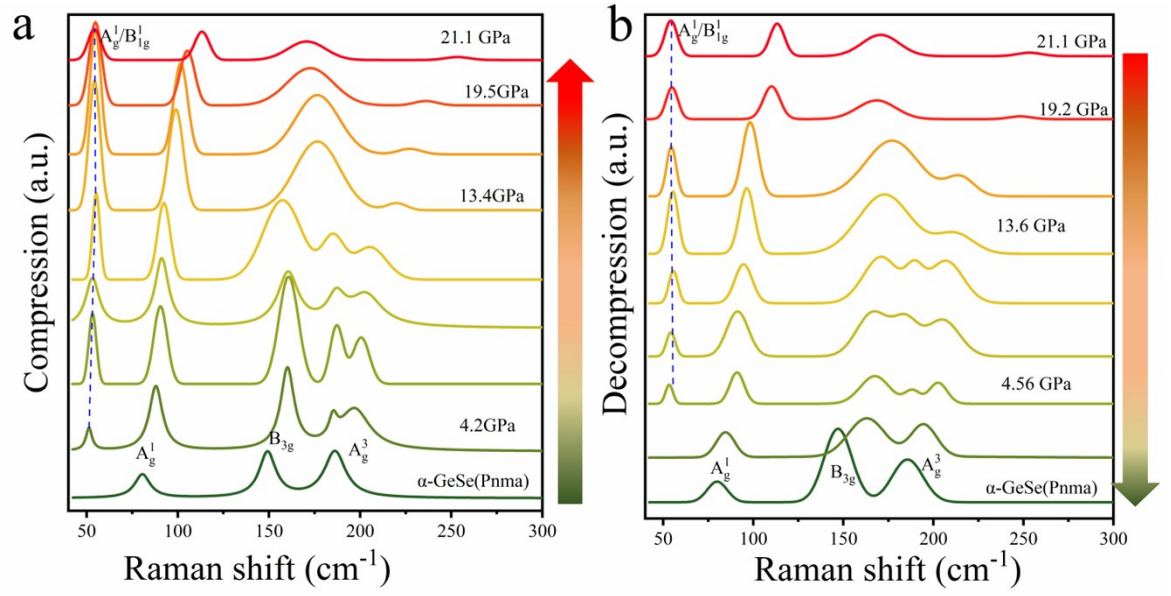

Figure S5. In situ Raman spectroscopy results. (a) High-pressure Raman spectra of *α*-GeSe from ambient pressure to 21.1 GPa. Silicone oil as pressure transmission medium. (b) Decompression-dependent Raman spectra of *α*-GeSe from 21.1 GPa to ambient pressure.

Controversy exists regarding the phase transition of the group IV−VI monochalcogenide GeSe under high pressure. To confirm the phase transition of *α*-GeSe under high pressure, we systematically studied the in-situ Raman spectra of two-dimensional van der Waals *α*-GeSe using different pressure transmission media. Additionally, we conducted further research on the phase transition during the decompression process. Figures S1 and S4 respectively show the Raman spectra and Raman mode dependence of *α*-GeSe under compression and decompression when silicone oil and sodium chloride are used as pressure transfer media. We observed the phase transition of *α*-GeSe from the *Pnma* to the *Cmcm* structure under hydrostatic pressure when the pressure reached up to 24 GPa. A new phase was successfully synthesized when pressure reached 4.7 GPa during decompression. Compared with silicone oil, sodium chloride exhibits a lower hydrostatic pressure environment, and *α*- GeSe does not undergo a phase transition from *Pnma* to *Cmcm* when pressure up to 21.1GPa. Additionally, no new phase is observed following decompression.

The two-dimensional van der Waals *α*-GeSe exhibits significant anisotropy, causing the Raman peak intensity of the sample to display pronounced angle dependence, regardless of whether polarizers in the optical path are added or not (Figure 1f and Figure2). So, we observed that angular dependence of the Raman mode of *α*-GeSe without polarizers when the pressure reached 28.1 GPa (Figure S2). When pressure up to 28.1 GPa, the anisotropy in GeSe completely vanishes, further confirming the phase transition from the *α-Pnma* phase to the *α-Cmcm* phase.

Table S1. Comparison of Raman modes and dv/dP(cm^{-1}GPa^{-1}) values of GeSe during the compression up to 28.12 GPa

v_0(cm^{-1})	pressure (GPa)	dvdp^{-1}	pressure (GPa)	dvdp^{-1}	pressure (GPa)	dvdp^{-1}	pressure (GPa)	dvdp^{-1}	Raman mode
47.91	0-10.2		10.2-13.6	0.088	13.2-22.6	0.075	22.6-28.1	0.195	A_g^1/B_{1g}^1

81.2	0-24.6	1.349	10.2-13.6	1.349	13.2-22.6	1.349	22.6-28.1	1.361	A_g^1
148.8	0-10.2	0.69	10.2-13.6	1.57	13.2-22.6	-0.56	22.6-28.1	0.21	B_{3g}
171.9	3.6-10.2	0.63	10.2-13.6	0.001	13.2-22.6		22.6-28.1		A_g^2
187.2	0-10.2	3.21	10.2-13.6	2.36	13.2-22.6	3.11	22.6-28.1	3.37	A_g^3

Table S2. Decompression of Raman modes and dv/dP($cm^{-1}GPa^{-1}$) values of GeSe from 28.12 GPa to atmospheric pressure

$v_0(cm^{-1})$	Pressure (GPa)	$dvdp^{-1}$	pressure (GPa)	$dvdp^{-1}$	Pressure (GPa)	$dvdp^{-1}$	Raman mode
47.91	28.1-4.6	-0.37					A^1_g/B^1_{1g}
81.2	28.12-0	-1.52					A^1_g
148.85			13.6-9.2	-2.3	9.2-0	-0.17	B_{3g}
178.23	28.12-13.6	0.03					
171.9			13.6-9.2	-0.68	9.2-0	-0.31	A^2_g
187.25	28.1-9.2	-1.58	9.2-0	-3.6			A^3_g
72.8	9.2-0	-1.22					New

During the decompression process of *α*-GeSe, it can be observed from the Raman spectra that the overlapping B_{3g} and A_g^2 modes split when the pressure is reduced to 13 GPa. After complete decompression, the peak positions of the A_g^1, B_{3g} and A_g^3 modes are observed to be nearly to their initial states (see Figure 3 and Figure S1). In addition, we observed a mixed region of *α-Pnma* and *β-Pnma* phase structures in the atomic structure using STEM (Figure S6)

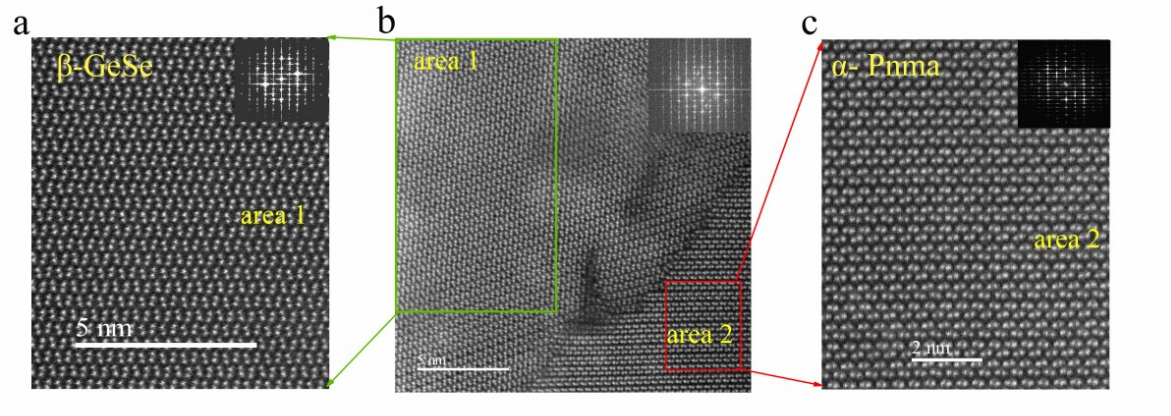

Figure S6. Structure characterization of GeSe after decompression. (a) The corresponding STEM images show area1 within region **b**. (b) STEM images for the mixture of *α*-GeSe and *β*-GeSe. (c) The corresponding STEM images show area2 within region **b**.

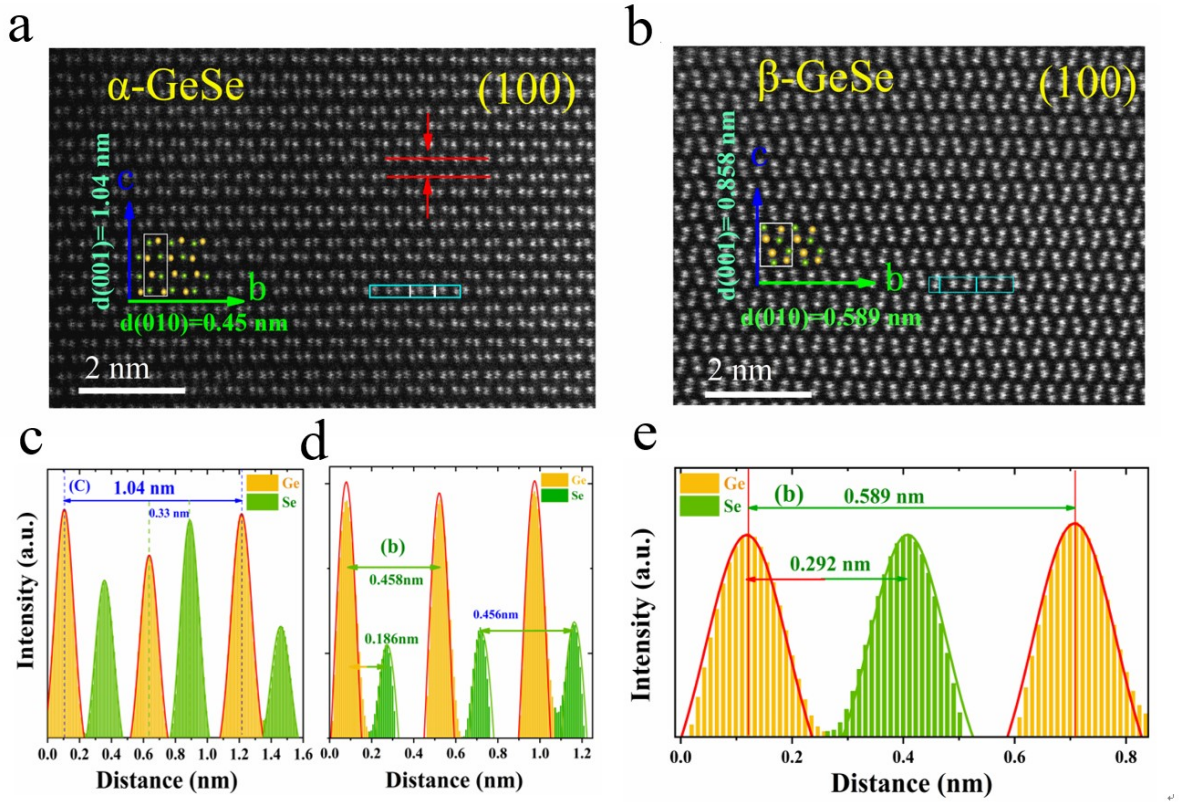

Figure S7. STEM images of the *Pnma* phase (a) and *β*-GeSe (b). The corresponding intensity line contours extracted from (a) reveal the spacing between (Ge-Se), (Ge-Ge), and (Se-Se) atom pairs along the c-axis (c) and b-axis (d). (e) The corresponding intensity contour extracted from (b) reveals the spacing between (Ge-Se), (Ge-Ge), and (Se-Se) atom pairs.

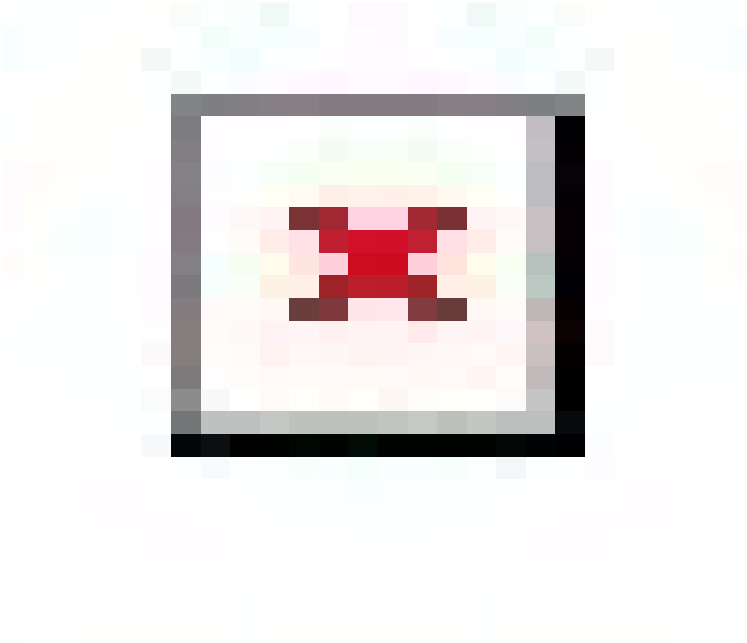

Figure S8. Photoluminescence spectra of *α*-GeSe under ambient conditions and *β*-GeSe following decompression from 28.12 GPa

Figures S7a and S7b are STEM images of different regions extracted from Figure S6b. Figure S7a shows the atomic structure and STEM image of the *α-Pnma* phase taken from [100] direction, revealing the atomic structure in the armchair (b-axis) direction. Figures S7c,d show the intensity line profiles of the c-axis (indicated by the blue line) and b-axis (indicated by the green line) in Figure S7a. It can be seen that a Ge-Ge atomic spacing of 1.04 nm and a Ge-Se atomic layer spacing of 0.33 nm along the c-axis, and a Ge-Ge atomic spacing of 0.458 nm and a Ge-Se atomic spacing of 0.186 nm along the b-axis. Therefore, the lattice parameters of the *α-Pnma* phase obtained after decompression are c=1.04 nm and b=0.458 nm. which are basically consistent with the lattice parameters of *α*-GeSe obtained from theoretical calculations and experiments. Figure 4a and Figure S7b shows the atomic structure and STEM image of the new phase taken from [100] direction, revealing the atomic structure in the armchair (b-axis) direction. In Figure S7b, It can be seen that a Ge-Ge atomic spacing of 0.858 nm along the c-axis, and a Ge-Ge atomic spacing of 0.589 nm along the b-axis. According to the STEM image, it is observed that the proportion of *α*- Gese in the mixed region is relatively small. The results indicate that subsequent to decompression, a minor segment of the region demonstrates a reversible phase transition from *α-Cmcm* to *α-Pnma*. In contrast, the overwhelming majority of the area undergoes a transformation to the *β*-GeSe. This phenomenon underscores the critical importance of pressure conditions in determining the phase transition of the GeSe structure.

Table S3. Summary of the phase transition in *α*-GeSe after compression and decompression under various pressure

Compression(GPa)	Pressure medium	Hydrostatic	Phase transition or note	After decompression
18.6	NaCl	none	None	α-GeSe
21.1	silicone oil	none	None	α-GeSe
24.6	silicone oil	none	Yes (Pnma to Cmcm)	β-GeSe
28.2	silicone oil	none	Yes (Pnma to Cmcm)	β-GeSe

Table S4 The Hydrostatic-Pressure properties of commonly utilized pressure transmission media

Type	Medium	Hydrostatic properties(300k)	Hydrostatic properties(77k)	In this experiment	Ref.
Ⅰ-type pressure medium	NaCl	100Kbar< good	Poor	yes	Adams,D.M, et al.1973[8]
	Silicon oil	4GPa< good	Poor	yes	Welber, B.1979[9]
	Vaseline	3GPa< good	Poor		Barnett, J.D et al.1973[10]
Ⅱ-type pressure medium	isopropanol	5GPa< good	5GPa< good		Decker D, et al. 1970.
	glycerol	5GPa< good	5GPa< good		Finger.L.W,1981[11]
Ⅱ-type pressure medium	N-pentane and Isopentane (1:1)	0 10GPa< good	5GPa< good		Piermarini,, et al. (1973)[12]
	Methanol and ethanol (4:1)	0 10GPa< good	5GPa< good	yes	Piermarini,, et al. (1973)[12]
	argon	13GPa	good		Bell and Mao (1982)[13]
	neon	20GPa	good		Bell and Mao (1978),[14]
	helium	30GPa	good		Bell and Mao (1978)[14]

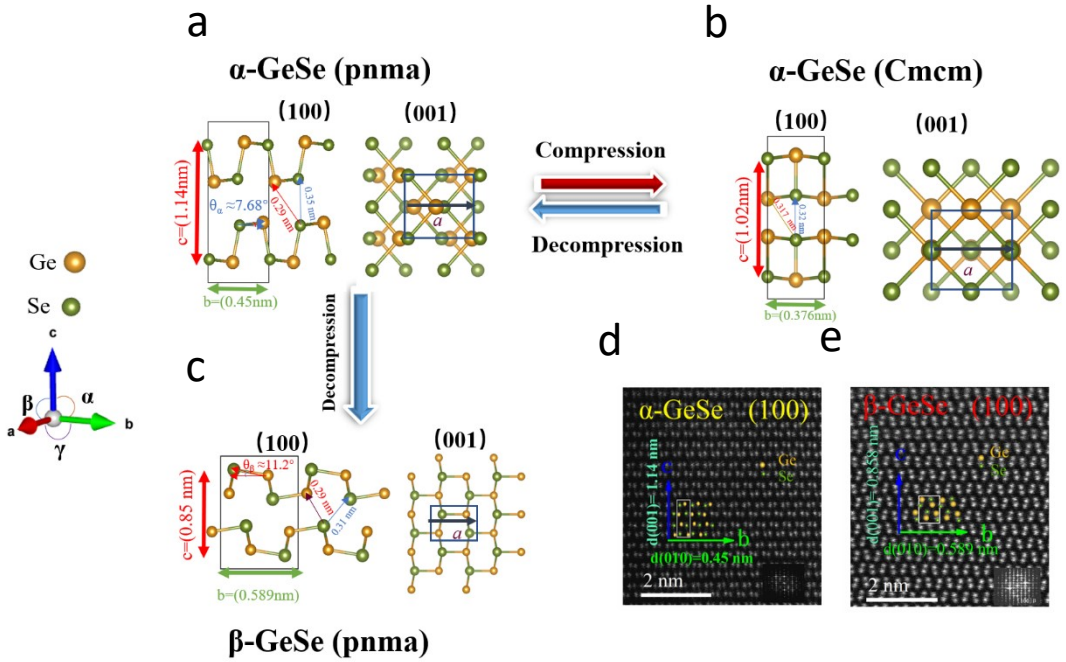

Figure S9. Schematic diagram of the phase transition from *α*-GeSe to *β*-GeSe. a) Atomic structure of the *α*-GeSe (*Pnma*) phase at ambient temperature and pressure. b) Atomic structure of the *α*-GeSe (*Cmcm*) phase under high pressure and ambient temperature. c) Atomic structure of *β*-GeSe (*Pnma*) observed after decompression from 24.6 GPa. Under pressure, a phase transition from *α-Pnma* to *α-Cmcm* occurs when the pressure reaches 24 GPa. Upon decompression from pressures greater than 24 GPa, the *α-Pnma* phase emerges around 13 GPa, and further decompression leads to the formation of *β*-GeSe, also in the Pnma space group. d) and e) show STEM images of *α*-GeSe and *β*-GeSe, respectively, before and after the pressure changes.

Reference

(1) Chen, X. L., Pengchao. Wang, Xuefei. Zhou, Yonghui. An, Chao. Zhou, Ying. Xian, Cong. Gao, Hao. Guo, Zhaopeng. Park, Changyong. Hou, Binyang. Peng, Kunling. Zhou, Xiaoyuan. Sun, Jian. Xiong, Yimin. Yang, Zhaorong. Xing, Dingyu. Zhang, Yuheng. *Phys. Rev. B*, 2017, **96**(16), 165123.

(2) von Rohr, F. O.; Ji, H.; Cevallos, F. A.; Gao, T.; Ong, N. P.; Cava, R. J. *J Am Chem Soc*, 2017, **139**(7), 2771-2777.

(3) Xu, Y. Z., Hao. Shao, Hezhu. Ni, Gang. Li, Jing. Lu, Hongliang. Zhang, Rongjun. Peng, Bo. Zhu, Yongyuan. Zhu, Heyuan. Soukoulis, Costas M. *Phys. Rev. B*, 2017, **96**(24), 245421.

(4) Xu, Y.; Xu, K.; Ma, C.; Chen, Y.; Zhang, H.; Liu, Y.; Ji, Y. *Journal of Materials Chemistry A*, 2020, **8**(37), 19612-19622.

(5) Bellin, C. P., A. Paulatto, L. Beneut, K. Biscaras, J. Narayana, C. Polian, A. Late, D. J. Shukla, A. *Phys Rev Lett*, 2020, **125**(14), 145301.

(6) Akifumi Onodera, I. S, and Yasuhiko Fujii. *Phys. Rev. B*, 1997, **56**, 7935.

(7) Cheng, H.; Yao, H.; Xu, Y.; Jiang, J.; Yang, Y.; Wang, J.; Li, X.; Li, Y.; Shao, J. *Chemistry of Materials*, 2024, **36**(8), 3764-3775.

(8) Payne, D. M. A. a. S. J. *Applied Spectroscopy*, 1973, **27**(5), 377.

(9) Welber, B.; Jayaraman, A. *Journal of Applied Physics*, 1979, **50**(1), 462-466.

(10) Barnett, J. D.; Block, S.; Piermarini, G. J. *Review of Scientific Instruments*, 1973, **44**(1), 1-9.

(11) Finger, L. W.; Hazen, R. M.; Zou, G.; Mao, H. K.; Bell, P. M. *Applied Physics Letters*, 1981, **39**(11), 892-894.

(12) Piermarini, G. J.; Block, S.; Barnett, J. D. *Journal of Applied Physics*, 1973, **44**(12), 5377-5382.

(13) Boctor, N. Z. B., P.M.; Mao, H.K.; Kullerud, G. *Geochimica et Cosmochimica Acta*, 1982, **46**(10), 1903-1911.

(14) Mao, H. K. *Science*, 1978, **200**(4346), 1145-1147.